SDSS1133: an unusually persistent transient in a nearby dwarf galaxy

Michael Koss,[1,2]⋆† Laura Blecha,[3]‡ Richard Mushotzky,[3] Chao Ling Hung,[2]
Sylvain Veilleux,[3] Benny Trakhtenbrot,[1]§ Kevin Schawinski,[1] Daniel Stern,[4]
Nathan Smith,[5] Yanxia Li,[2] Allison Man,[6] Alexei V. Filippenko,[7] Jon C. Mauerhan,[5]
Kris Stanek[8] and David Sanders[2]

[1]*Institute for Astronomy, Department of Physics, ETH Zurich, Wolfgang-Pauli-Strasse 27, CH-8093 Zurich, Switzerland*
[2]*Institute for Astronomy, University of Hawaii, 2680 Woodlawn Drive, Honolulu, HI 96822, USA*
[3]*Astronomy Department, University of Maryland, College Park, MD 20742, USA*
[4]*Jet Propulsion Laboratory, California Institute of Technology, 4800 Oak Grove Drive, MS 169-506, Pasadena, CA 91109, USA*
[5]*Steward Observatory, University of Arizona, 933 N. Cherry Ave., Tucson, AZ 85721, USA*
[6]*Dark Cosmology Center, University of Copenhagen, DK-2100 Copenhagen, Denmark*
[7]*Department of Astronomy, University of California, Berkeley, CA 94720-3411, USA*
[8]*Department of Astronomy, The Ohio State University, Columbus, OH 43210, USA*

ABSTRACT

While performing a survey to detect recoiling supermassive black holes, we have identified an unusual source having a projected offset of 800 pc from a nearby dwarf galaxy. The object, SDSS J113323.97+550415.8, exhibits broad emission lines and strong variability. While originally classified as a supernova (SN) because of its non-detection in 2005, we detect it in recent and past observations over 63 yr and find over a magnitude of rebrightening in the last 2 yr. Using high-resolution adaptive optics observations, we constrain the source emission region to be $\lesssim 12$ pc and find a disturbed host-galaxy morphology indicative of recent merger activity. Observations taken over more than a decade show narrow [O III] lines, constant ultraviolet emission, broad Balmer lines, a constant putative black hole mass over a decade of observations despite changes in the continuum, and optical emission-line diagnostics consistent with an active galactic nucleus (AGN). However, the optical spectra exhibit blueshifted absorption, and eventually narrow Fe II and [Ca II] emission, each of which is rarely found in AGN spectra. While this peculiar source displays many of the observational properties expected of a potential black hole recoil candidate, some of the properties could also be explained by a luminous blue variable star (LBV) erupting for decades since 1950, followed by a Type IIn SN in 2001. Interpreted as an LBV followed by an SN analogous to SN 2009ip, the multidecade LBV eruptions would be the longest ever observed, and the broad Hα emission would be the most luminous ever observed at late times (>10 yr), larger than that of unusually luminous SNe such as SN 1988Z, suggesting one of the most extreme episodes of pre-SN mass-loss ever discovered.

Key words: supernovae: general – galaxies: active – galaxies: dwarf.

1 INTRODUCTION

The coalescence of binary supermassive black holes (SMBHs) in galaxy mergers is thought to constitute the strongest source of gravitational waves (GW; Merritt & Milosavljević 2005). Theory suggests that these waves carry momentum, causing the merged black hole (BH) to experience a velocity recoil or kick that displaces it from the centre of its host galaxy (Peres 1962; Bekenstein 1973; Thorne & Braginskii 1976). Numerical simulations of SMBH mergers have found, surprisingly, that GW recoil kicks may be quite large, up to $\sim$5000 km s^{-1} (Campanelli, Lousto & Zlochower 2006; Lousto & Zlochower 2011). Consequently, a merged SMBH may even be ejected from its host galaxy.

An active galactic nucleus (AGN) ejected from the centre of a galaxy should be able to carry along its accretion disc as well as the broad-line region, resulting in an AGN spatially offset from its

host galaxy and/or an AGN with broad emission lines offset in velocity (Madau & Quataert 2004; Blecha & Loeb 2008; Komossa & Merritt 2008). Recoiling AGNs with offsets >1 kpc may have lifetimes up to tens of Myr for a fairly wide range in kick speeds, and velocity-offset AGNs may have similar lifetimes (Blecha et al. 2011, 2013). Thus far, several candidate recoiling SMBHs have been found via spatial offsets, though none has been confirmed (see Komossa 2012 for a review). The disturbed galaxy CXOC J100043.1+020637 (or CID-42) contains a candidate recoiling AGN offset by 2.5 kpc from the galactic centre (Civano et al. 2010, 2012). However, in order for the recoiling AGN to produce narrow-line emission, it must be observed very quickly after the kick while it still inhabits a dense gaseous region. Another recoil candidate found by Jonker et al. (2010) consists of an X-ray source offset by 3 kpc from the centre of an apparently undisturbed spiral galaxy, but this could also be explained as an ultraluminous X-ray source (ULX) associated with an accreting intermediate-mass black hole (IMBH) in a massive, young stellar cluster, or perhaps a very luminous Type IIn supernova (see Filippenko 1997 for a review).

These recoiling kicks have significant implications for models of SMBH and galaxy coevolution (Volonteri 2007; Blecha et al. 2011; Sijacki, Springel & Haehnelt 2011). A hitherto unknown low-redshift population of SMBH mergers in dwarf galaxies could have profound implications for GW detectors. Although the SMBH occupation fraction in dwarf galaxies is uncertain, their shallower potential wells greatly increase the possibility of detecting GW kicks; nearly every major SMBH merger would result in a substantial displacement of the remnant SMBH. While current detectors, like the advanced *Laser Interferometer Gravitational-Wave Observatory* or Pulsar Timing Arrays, are more sensitive to stellar-mass BHs or the most massive SMBHs (Sesana 2013), future space-based detectors such as the proposed Laser Interferometer Space Antenna would be more sensitive to lower mass SMBHs ($\sim 10^5$–10^6 M$_\odot$), making this mass range found in dwarf galaxies an important population for study.

Particularly at low bolometric luminosities ($L_{bol} \leq 10^{43}$ erg s^{-1}), some SNe IIn can be a source of imposters for AGNs (Filippenko 1989) and recoiling SMBHs, especially when the broad-line emission lasts for decades. Some SNe are also preceded by strong winds and non-terminal eruptions similar to those of luminous blue variables (LBVs) such as η Carinae (Smith et al. 2011). There is also evidence that LBV eruptions can be followed by SNe IIn (Gal-Yam et al. 2007; Mauerhan et al. 2013; Ofek et al. 2014), with narrow as well as broader Balmer emission lines that can persist for decades (Smith et al. 2008b; Kiewe et al. 2012), sometimes with an appearance similar to that of broad-line AGNs. SNe IIn occur in a dense circumstellar medium (CSM) created by pre-SN mass-loss, and the narrow hydrogen lines are produced by photoionization of the dense winds irradiated by X-rays from the region behind the forward shock (Chevalier & Fransson 1994). (The broader lines arise when the SN ejecta interact directly with the CSM.) Type IIn SNe can even produce forests of narrow coronal lines such as [O III] (e.g. SN 2005ip; Smith et al. 2009).

Our study focuses on an enigmatic point source, SDSS J113323.97+550415.8 (hereafter SDSS1133), having a projected offset of 800 pc (5.8 arcsec) from the centre of a nearby dwarf galaxy, Mrk 177 (UGC 239), and with broad-line emission observed by the Sloan Digital Sky Survey (SDSS) in 2003. SDSS1133 was mentioned as a possible case of a quasar having a non-cosmological redshift because of its broad Balmer lines but very low luminosity (López-Corredoira & Gutiérrez 2006). In a study of narrow-line Seyfert 1 galaxies, Zhou et al. (2006) classified SDSS1133 as an

SN because of its non-detection in data obtained in January 2005 with the 2.16-m telescope at the Beijing Observatory. This SN classification was also applied by Reines, Greene & Geha (2013) based on the SDSS spectra using the automated SN detection code of Graur & Maoz (2013). Finally, SDSS1133 was listed as a possible 'Voorwerp' candidate for a giant ionized cloud (Keel et al. 2012).

To better understand this unusual source, we obtained new optical spectra, adaptive optics (AO) images, and ultraviolet (UV) and X-ray observations of it. We also analysed archival images, finding that the object is detected over a time span of 63 yr. The host galaxy, Mrk 177, is at a distance of 28.9 Mpc (distance modulus 32.3 mag; Tully 1994). We use this redshift-independent distance indicator for the subsequent analysis of SDSS1133 and Mrk 177. At this distance, 1 arcsec corresponds to 140 pc. Galactic foreground extinction is very low, $A_V = 0.03$ mag (Schlafly & Finkbeiner 2011).

2 OBSERVATIONS AND DATA ANALYSIS

2.1 Imaging

We use archival optical SDSS images from 2001 December 18 and 2002 April 1 (UT dates are used throughout this paper), as well as 111 *griz* images taken over 26 nights from Pan-STARRS1 (PS1) between 2010 March and 2014 March. Additionally, we have photographic Digital Sky Survey (DSS) plates from the POSS I and II surveys, with 1 arcsec pixel^{-1} sampling and a limiting magnitude of 21 and 22.5, respectively. The 1994 observation, with the IIIaJ emulsion and GG395 filter, is comparable to the *g* filter. The 1950 plate from the POSS-I O survey uses the 103aO emulsion with a response between *u* and *g*. The 1999 observation is with the IIIaF emulsion, similar to the *i* band. Example images can be found in Fig. 1 with measurements in Table 1.

We measure the photometry of SDSS1133 (Figs 2 & 3) using a two-dimensional surface brightness fitting program, GALFIT (Peng et al. 2002). We fit a 5 arcsec region around SDSS1133, using a point spread function (PSF) model for the source light and a linear model based on radial distance to model contamination from Mrk 177. The PSF model position is allowed to vary across the image region. PSF models from the SDSS and PS1 data are used for the image convolution. For the PSF model in DSS images, we use a median of five nearby, bright, unsaturated stars. The DSS imaging scale is in photographic density, which is non-linear with intensity. Thus, the increase in contamination from the galaxy causes the source intensity to be underestimated. To correct for this non-linearity in DSS images, we measure SDSS PSF magnitudes of five nearby unsaturated stars with varying brightnesses to calculate the magnitude of SDSS1133 in the DSS plates.

We fit the positions of five bright, unsaturated stars common to each of the images for source astrometry, using the 2001 SDSS astrometry as the reference. We find no significant difference between SDSS and PS1 astrometry. For the DSS images, the declination offsets are <0.2 arcsec with respect to the SDSS astrometry, while we find right ascension offsets of 1 arcsec in the 1950 DSS image and 0.6 arcsec in the 1994 image.

We also estimate photometry from SDSS spectra taken in 2003 March using PYSYNPHOT, which determines the flux in the spectra as measured by different photometric filters. We convert from spectra filter magnitudes to PSF magnitudes using the offset between fiber-mag and PSF magnitudes from the original SDSS images. Finally, we include as an upper limit an observation in 2005 January using the 2.16-m telescope of the Beijing Observatory which failed to
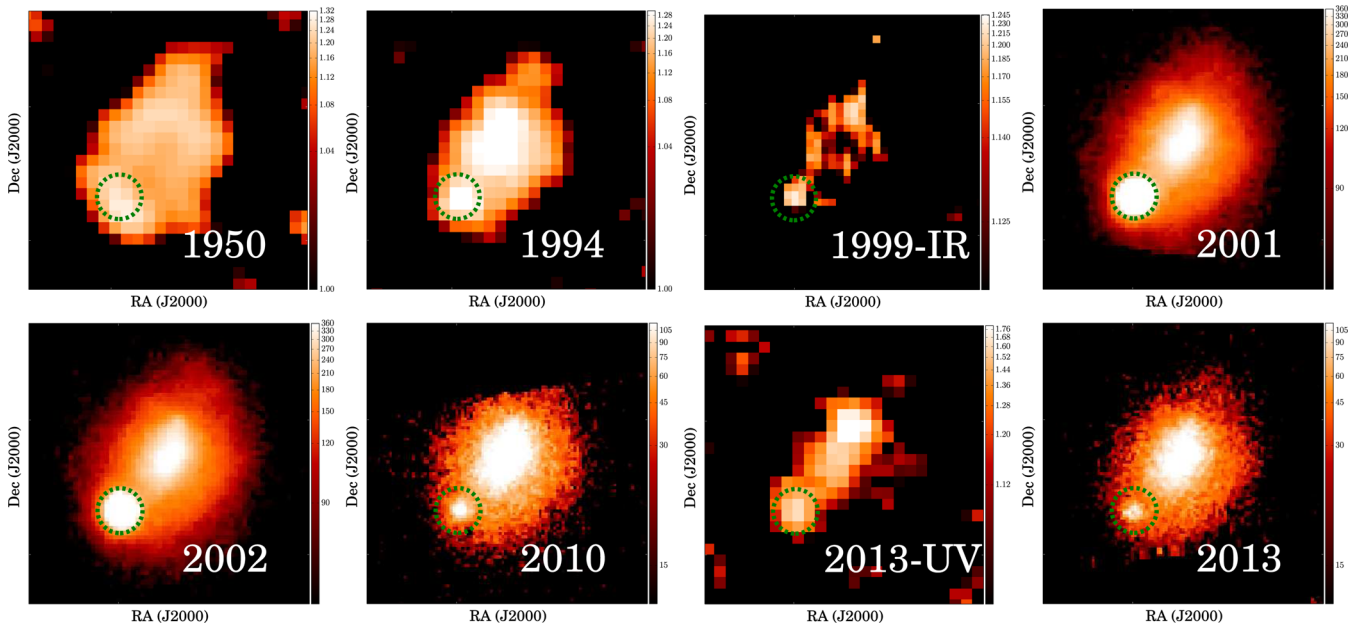
Figure 1. Images of the host galaxy Mrk 177 and SDSS1133, 25 arcsec wide and displayed with an arcsinh scale representing photographic density or CCD counts. The 1950 and 1994 images are from blue DSS plates, the 1999 image is from an IR DSS plate, and the 2001–2013 data are *g*-band images from the SDSS and PS1. A dashed green circle of 2 arcsec radius is drawn for SDSS1133 based on positions in the 2001 SDSS observation. A 3-pixel unsharp mask has been applied to the DSS and UV images because of their lower resolution and pixel sampling.

detect the source within 3 mag of the 2002 SDSS observation (Zhou et al. 2006).

We obtained AO images on 2013 June 16 with the Near Infrared Camera 2 (NIRC2) instrument on the Keck-2 10-m telescope equipped with the wide camera, which has a 40 arcsec field of view (FOV) and 40 mas pixel^{-1} (Fig. 4). In this observation, we used a three-point dither pattern for 6 min in the *J* and K_p filters, as well as 12 min in the Paβ filter. The Paβ filter covers the redshift of SDSS1133 and Mrk 177 ($z = 0.007\,845$). An image of the AO tip-tilt star is used for PSF estimation (Fig. 5) and photometric calibration based on measured 2MASS magnitudes in *J* and K_p.

The *Swift* satellite observed SDSS1133 as a Target of Opportunity (ToO) programme on 2013 August 26, 27, and 28 for 3.5, 3.8, and 11.2 ks, respectively, with its X-Ray Telescope (XRT) in Photon Counting mode (PC mode) and the UV-Optical Telescope (UVOT) with the *UVW*1 near-UV filter. The total exposure time was 18.5 ks. X-ray data were reduced with the task XRTPIPELINE (version 0.12.6). Source and background photons were extracted with XSELECT (version 2.4b), from circles with radii of 47 and 200 arcsec, respectively, in the 0.3–10 keV band. For PSF photometry with UVOT, we use a nearby star with known magnitudes scaled to the brightness of SDSS1133.

2.2 Optical Spectroscopy

We use optical spectra from a variety of telescopes for this study of SDSS1133 (Figs 6–8). SDSS spectra were taken in 2003 March, 456 d after the object had diminished in brightness about 2.5 mag from its peak in 2001 December. SDSS1133 was targeted as part of the *ugri*-selected quasar survey because of its AGN-like colours.

SDSS1133 was also observed with the University of Hawaii 2.2-m telescope and the SuperNova Integral Field Spectrograph (SNIFS) on 2013 May 1–4 for a total duration of 160 min. SNIFS is an optical integral field unit (IFU) spectrograph with blue (3000–

5200 Å) and red (5200–9500 Å) channels having a resolution of 360 km s^{-1}. The SNIFS reduction pipeline SNURP was used for wavelength calibration, spectro-spatial flat-fielding, cosmic ray removal, and flux calibration (Aldering et al. 2006). A sky image was taken after each source image and subtracted from each IFU observation. Flux corrections were applied each night based on the standard star Feige 34. In order to estimate the amount of narrow-line contamination from Mrk 177 at the position of SDSS1133 in the SDSS spectrum, we placed an aperture at the same radial distance from Mrk 177, but to the north-east of SDSS1133 with the same aperture size as the SDSS fibre (3 arcsec).

We used the DEep Imaging Multi-Object Spectrograph (DEIMOS) on the Keck-II telescope to obtain a 10 min spectrum (range 4730–9840 Å) of the object and the galaxy nucleus (2 arcsec slit, PA = 137°.5) with a 600 lines mm^{-1} grating on 2013 December 13. Finally, we used the Multiple Mirror Telescope (MMT) to observe SDSS1133 on 2014 January 3 (1 arcsec slit, PA = 137°.5); the spectrum spans 3700–8926 Å.

We fit the spectra using an extensible spectroscopic analysis toolkit for astronomy, PYSPECKIT, which uses a Levenberg–Marquardt algorithm for fitting. We adopt a power-law fit to model the continuum and Gaussian components to model the emission lines. All narrow-line widths were fixed to the best fit of the [O III] λ5007 line. We fit the spectra of Hα using a narrow component based on the [O III] λ5007 line along with a broad component. Additionally, some AGNs have broad Balmer lines that are poorly fitted with a single Gaussian component, so we fit Hα and Hβ with two broad components (broad and very broad) when it is statistically significant based on the reduced χ^2. Fitting the Hβ line is more complicated because of Fe II lines on the red wing as well as [O III] λ4959 on the red wing; we therefore use the Hβ fitting procedure following the code described by Trakhtenbrot & Netzer (2012). To measure the full width at half-maximum intensity (FWHM) of the broad component of the Balmer lines, we first subtract the narrow-line component. Finally, we fit a separate broad component

Table 1. Photometry.

Filter[a]	Mag[b]	Mag err[c]	Date	Telescope[d,e]	
103aO	18.6	0.7	1950-03-20	DSS1	1
IIIaJ	18.4	0.40	1994-04-14	DSS2	1
IIIaF	18.8	0.50	1999-04-25	DSS2	1
u	16.28	0.08	2001-12-18	SDSS	1
u	16.75	0.08	2002-04-01	SDSS	1
g	16.41	0.04	2001-12-18	SDSS	1
g	16.40	0.04	2002-04-01	SDSS	1
g	18.7	0.18	2003-03-09	SDSSspec	1
i	16.48	0.04	2001-12-18	SDSS	1
i	16.40	0.04	2002-04-01	SDSS	1
i	18.65	0.05	2003-03-09	SDSSspec	1
r	16.26	0.04	2001-12-18	SDSS	1
r	16.31	0.04	2002-04-01	SDSS	1
r	18.28	0.06	2003-03-09	SDSSspec	1
z	16.45	0.04	2001-12-18	SDSS	1
z	16.34	0.04	2002-04-01	SDSS	1
z	18.49	0.08	2003-03-09	SDSSspec	1
NUV	21.62	0.40	2004-03-06	*GALEX*	1
g	19.4	0.0	2005-01-01	Beijing	1
g	19.58	0.01	2010-03-17	PS1	4
g	19.68	0.05	2011-03-12	PS1	8
g	20.18	0.01	2012-02-22	PS1	2
g	19.38	0.07	2013-01-16	PS1	8
r	19.02	0.03	2010-03-13	PS1	4
r	19.37	0.01	2011-03-12	PS1	4
r	19.91	0.04	2012-02-22	PS1	4
r	19.31	0.06	2012-12-27	PS1	4
r	19.49	0.02	2013-02-09	PS1	8
r	19.02	0.03	2014-03-24	PS1	4
i	19.48	0.03	2010-03-03	PS1	4
i	19.5	0.03	2011-03-14	PS1	4
i	20.12	0.03	2012-02-11	PS1	4
i	19.62	0.04	2013-01-27	PS1	4
i	19.48	0.03	2014-03-16	PS1	4
z	19.43	0.07	2010-02-27	PS1	8
z	19.72	0.03	2010-05-18	PS1	8
z	19.57	0.01	2010-12-25	PS1	4
z	19.73	0.10	2011-01-22	PS1	4
z	19.82	0.01	2011-05-11	PS1	4
z	20.11	0.12	2012-02-09	PS1	4
z	19.82	0.02	2012-04-10	PS1	4
z	19.48	0.02	2013-01-03	PS1	4
z	19.32	0.05	2014-01-20	PS1	1
J	19.02	0.18	2013-06-16	NIRC2	1
Kp	18.92	0.16	2013-06-16	NIRC2	1
UVW1	21.41	0.30	2013-08-27	SWIFT	1
g	19.19	0.20	2014-01-04	MMTspec	1

[a]Specific filter used for image. The 103aO, IIIaJ, and IIIaF designations refer to plates from the DSS.

[b]All magnitudes are listed as AB mag.

[c]Uncertainty from photometric zero-point and uncertainty in measuring photometry with GALFIT. For synthetic photometry from spectra, the uncertainty includes the conversion from aperture to PSF magnitudes.

[d]MMTspec and SDSSspec indicate synthetic photometry; all of the other observations were from imaging.

[e]Number of observations taken at separate times within 1 week of the first observation. For PS1 several observations are often taken within a week; we have measured the weighted mean of these separate observations.

to each of the calcium near-infrared (NIR) triplet ($\lambda\lambda 8498$, 8452, 8662) lines and to O I $\lambda 8446$. The luminosities of the narrow lines and their velocity offsets from Mrk 177 can be found in Table 2.

3 RESULTS

3.1 X-ray, UV, optical, and NIR emission

Imaging from multiple time periods can differentiate an AGN from an SN; the latter typically fade quickly, and they rapidly become redder in colour. Using images from the DSS, SDSS, and the PS1 survey (Fig. 1) along with synthetic photometry from the observed spectra, we measure the *g* mag of SDSS1133 between 1950 and 2013 (Fig. 2). We find that SDSS1133 brightened in 2001 and 2002 compared to 1950 and 1993, and it shows variable brightening and dimming between 2010 and 2013. A non-detection in a 2MASS image on 2000 January 10, in the NIR, suggests that significant brightening happened sometime between 2000 January 10 and the first SDSS image on 2001 December 18. SDSS1133 was detected in the near-UV at −10.7 mag AB in 2004 and at −10.9 mag AB in 2013 by the *GALEX* and *Swift* satellites (respectively), 2 and 12 yr after peak brightness (assumed to be the first SDSS observation on 2001 December 18). Over the last 12 yr, the optical and UV colours of SDSS1133 have remained relatively constant (Fig. 2, right) and consistent with those of quasars (Richards et al. 2001).

High-resolution imaging at the $\lesssim 20$ pc scale is critical for differentiating between an ongoing merger of two galaxies and a post-merger recoiling SMBH that has left its host-galaxy nucleus behind. We imaged a 40 arcsec region around SDSS1133 in the NIR Paβ and K_p filters using AO with the NIRC2 instrument on the Keck-II telescope (Fig. 4). The images reveal an unresolved point source at spatial scales of $\lesssim 12$ (K_p) and $\lesssim 22$ pc (Paβ) coincident with the location of SDSS1133. SDSS1133 shows average colours ($g - i \approx -0.3$ to 0.2 mag) constant within the uncertainties from 2002 to 2014. This colour is consistent with nearby ($z < 0.1$) SDSS quasars (Richards et al. 2001). Additionally, the $i_{AB} - K_{Vega}$ colour of SDSS1133 is 2.5 mag, in agreement with results for low-redshift quasars (Peth, Ross & Schneider 2011) and much redder than the stellar locus ($i - K \approx 1$ mag). While red colours can be found in SNe because of dust formation, these colours often evolve with time.

NIR images trace the old stellar population and the bulk of the stellar mass. Those of SDSS1133 exhibit a disturbed morphology and a double-nucleus structure with a separation of 60 pc. The K_p absolute magnitudes of the nuclei are −14.1 and −14.2, in the range of dwarf-galaxy nuclei or very young, massive star clusters (Forbes et al. 2008). Radial profiles of SDSS1133 and the tip-tilt star used in each observation are shown in Fig. 5. The radial profiles of the nuclei in K_p and Paβ are consistent with the stellar profiles of the tip-tilt stars, suggesting no extended emission.

With the *Swift* XRT at 0.3–10 keV, 7.6 ± 3.4 background-subtracted counts were detected, corresponding to a signal-to-noise ratio (S/N) of 2.2 and a net count rate of $(4.1 \pm 1.8) \times 10^{-4}$ counts s^{-1}. The marginal *Swift* X-ray detection cannot distinguish between the AGN and SN scenarios. Assuming a power-law index of 1.9, representative of an AGN, the luminosity is 1.5×10^{39} erg s^{-1} in the 0.3–10 keV band.

3.2 Spectral shape, narrow-line diagnostics, broad-line emission

We measure the amount of narrow-line emission detected in SDSS1133, the nucleus of the host galaxy Mrk 177, and at a position the same radial distance from the nucleus of Mrk 177 as SDSS1133 (Mrk 177 IFU-offset) using the IFU image; the latter allows us
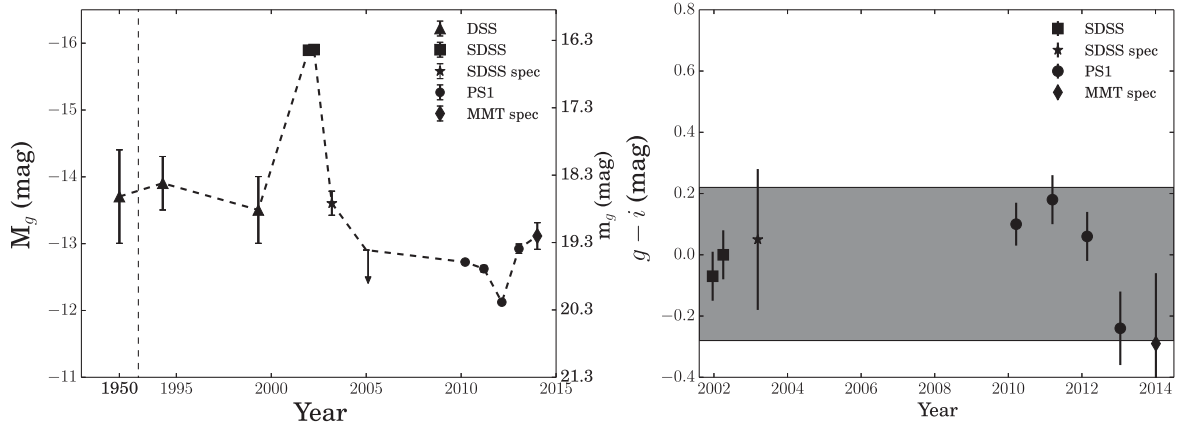
Figure 2. Left: measured *g* magnitudes for SDSS1133 over the last 63 yr from DSS photographic plates, the SDSS, and PS1. The vertical dashed line indicates a time gap. The blue DSS filter magnitudes have been converted to *g* magnitudes based on the SDSS colours. The 2005 observation represents an upper limit. We also included lower quality synthetic photometry taken from the SDSS and MMT spectroscopy in time periods where higher quality photometry was not available. Right: measured *g* − *i* colours of SDSS1133 since its peak brightness in 2001. Photometry is from the SDSS and PS1 during 2010–2014. We also included lower quality synthetic photometry taken from the SDSS and MMT spectroscopy in time periods where higher quality photometry was not available. The grey shaded region indicates average colours of nearby ($z < 0.1$) SDSS quasars (Richards et al. 2001).
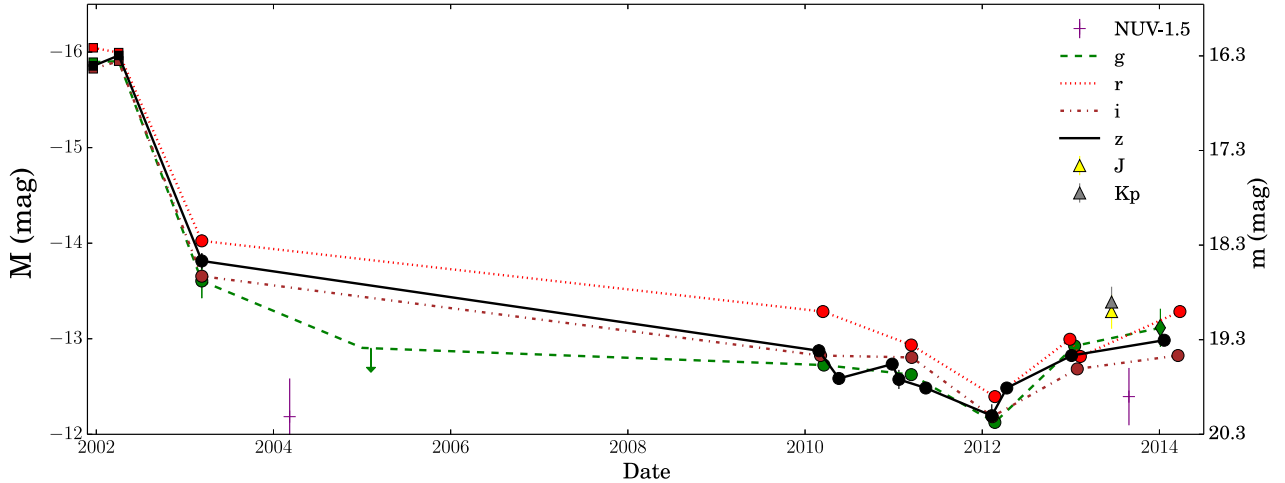
Figure 3. Photometry of SDSS1133 since its peak brightness in 2001 in AB mag. Optical observations (*griz*) are shown for the first year in 2001–2002 from the SDSS (filled squares), an upper limit from the Beijing observatory in 2005 (arrow), and finally observations from PS1 in 2010–2014 (filled circles). Error bars are typically smaller than symbols. We have also included lower quality synthetic photometry taken from the SDSS and MMT (stars) in time periods where higher quality photometry was not available. NIR AO observations from NIRC2 are shown as triangles. NUV *GALEX* and *Swift* UVOT data are shown as purple crosses and have been offset by 1.5 mag.

to determine the expected level of narrow-line contamination in SDSS1133 from Mrk 177. All line offsets are from the wavelength of [O III] $\lambda 5007$ in Mrk 177 at $z = 0.007\,845$. The measured line offset of the narrow lines in SDSS1133 and the host galaxy, Mrk 177, is redshifted by a small amount (26 ± 9 km s^{-1}), while Mrk 177 IFU-offset is blueshifted by a small amount (-18 ± 12 km s^{-1}). The narrow-line FWHMs of SDSS1133 and Mrk 177 are consistent with the SDSS instrumental resolution (150 km s^{-1}). The FWHM of Mrk 177 IFU-offset is consistent with the spectral resolution of the IFU (360 km s^{-1}).

We apply AGN emission-line diagnostics (e.g. Veilleux & Osterbrock 1987; Kewley et al. 2006) to the [N II]/Hα, [S II]/Hα, [O I]/Hα narrow lines of SDSS1133 and Mrk 177 (Fig. 6). The host galaxy, Mrk 177, is classified as an H II region in all diagnostics. SDSS1133 is classified as a Seyfert with the [S II] and [O I] diagnostics in 2003 SDSS spectra.

We find that the [N II] luminosity of the narrow-line emission found in SDSS1133 in 2003 and 2013 is consistent with that of Mrk 177 IFU-offset. However, the [O III], Hβ, Hα, and [O II] lines are significantly stronger than in Mrk 177 IFU-offset. This is confirmed by the two-dimensional images, which show that the emission lines are above the continuum level of SDSS1133 and Mrk 177. By 2013, the [O III] luminosity decreased.

A plot of the Hβ spectral region can be found in Fig. 7. We see that the 2013 Keck spectrum exhibits narrow Fe II emission, less-broad Hβ emission (2020 versus 2530 km s^{-1}), lower luminosity, weaker continuum emission, and a lower intensity ratio of [O III] to Hβ compared to the 2003 spectrum. Examining Hα in 2013 (Fig. 8), we find wider broad Hα emission (1390 versus 1660 km s^{-1}) and lower luminosity than in 2003. Assuming SDSS1133 is an AGN, we fit the Hβ region and measure an SMBH mass (Grier et al. 2013) of $\log(M_{BH}/M_\odot) \approx 6.0$, 6.0, and 6.2 in 2003, 2013, and 2014,
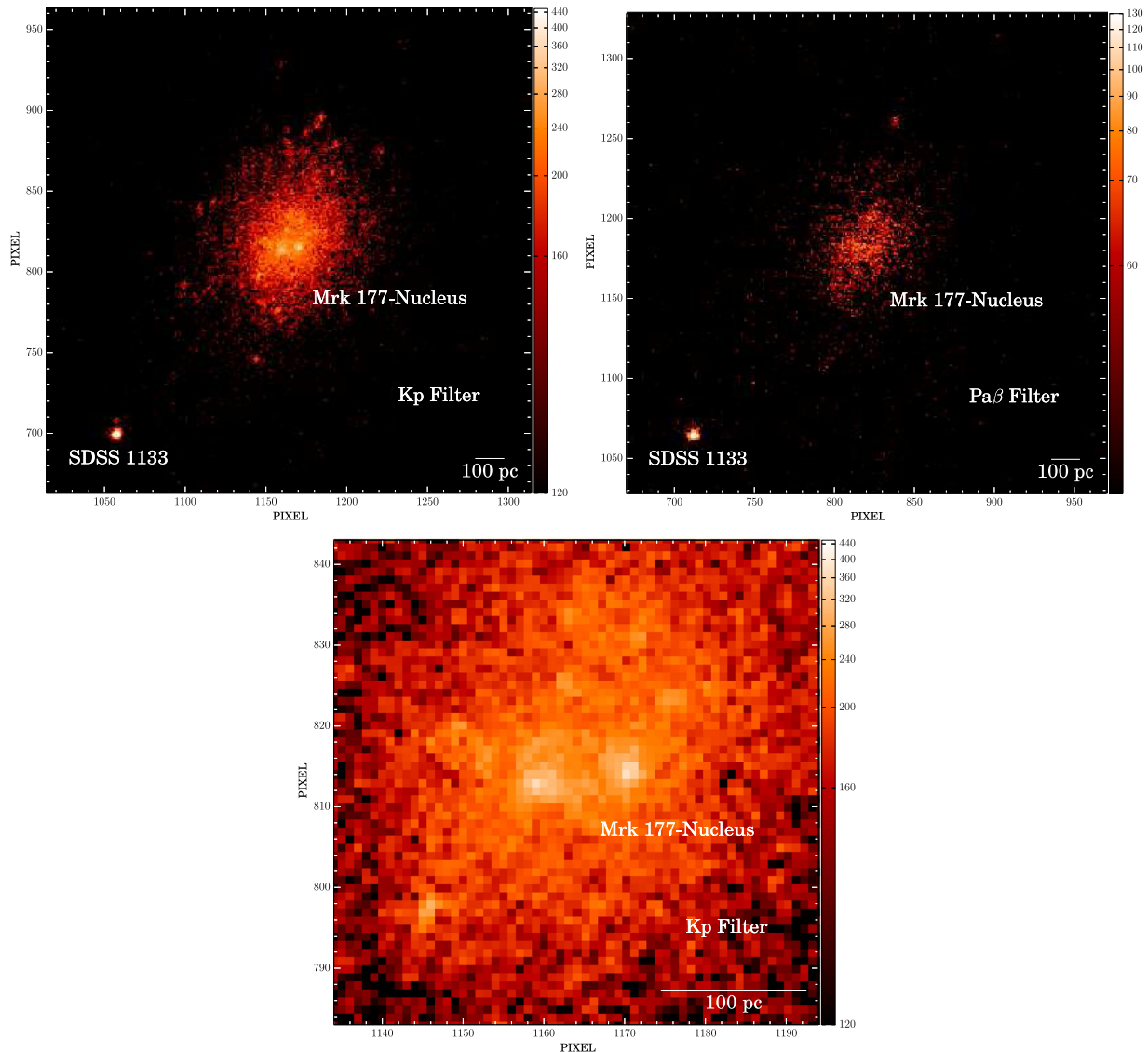
Figure 4. AO images of SDSS1133 and Mrk 177. The image is centred on Mrk 177 with a spatial scale of 40 mas pixel^{-1} and displayed with an arcsinh scale in CCD counts. Top-left: 12 arcsec wide K_p image. The FWHM of SDSS1133 is consistent with the PSF image (FWHM = 0.08 arcsec), corresponding to point-like emission at a scale of 12 pc. Top-right: 12 arcsec wide Paβ image. The FWHM of SDSS1133 is consistent with the PSF image (FWHM = 0.15 arcsec) corresponding to point-like emission at a scale of 22 pc. Bottom: 2.4″ K_p zoomed-in image of the nuclear region of Mrk 177 showing signs of morphological disruption and two nuclei.

respectively. Like all single-epoch ('virial') M_{BH} determinations, these estimated values have uncertainties of about 0.5 dex (Shen 2013), suggesting that the measured SMBH masses are constant within the uncertainties.

A plot of the broad Balmer lines smoothed to the same resolution and offset to the same continuum can be found in Fig. 9. There is evidence of blueshifted absorption in the Hβ and Hα regions at -3000 to -8000 km s^{-1}. The total broad Hβ emission dropped by 10–20 per cent between 2003 and 2013–2014, whereas the total broad Hα emission dropped by 65–70 per cent. The broad Hα/Hβ intensity ratio is 13 in 2003 and 5 in 2013–2014. The Balmer decrement in 2003 for the broad hydrogen lines is considerably larger than the recombination value, suggesting that the broad emission originates in very dense gas or suffers higher extinction. Finally, the change in blueshifted absorption, which is different in 2003 than

in 2013–2014, may cause variation in the broad-line emission and Balmer decrement.

A feature associated with the broad-line region in 1/3 of quasars (Netzer 1990) and some SNe is broad emission in the Ca II NIR triplet ($\lambda\lambda$8498, 8452, 8662) and O I λ8446 (Fig. 10). In 2003, we find the FWHM of these lines to be 630–650 km s^{-1}, significantly higher than that of the narrow-line region, and offset by 117 ± 36 km s^{-1} for the Ca II triplet and 210 ± 52 km s^{-1} for O I. The 2013 Keck spectrum exhibits narrower Ca II emission of 270 km s^{-1}. Fits to [Fe II] λ7155 and [Ca II] $\lambda\lambda$7291, 7324 show that no emission lines are detected in 2003, whereas the 2013 Keck spectrum exhibits strong, narrow emission consistent with the instrumental resolution (220 km s^{-1}).

We fit the spectrum blueward of 5000 Å and find a best fit for a possible non-thermal power-law AGN contribution (λ^p) of
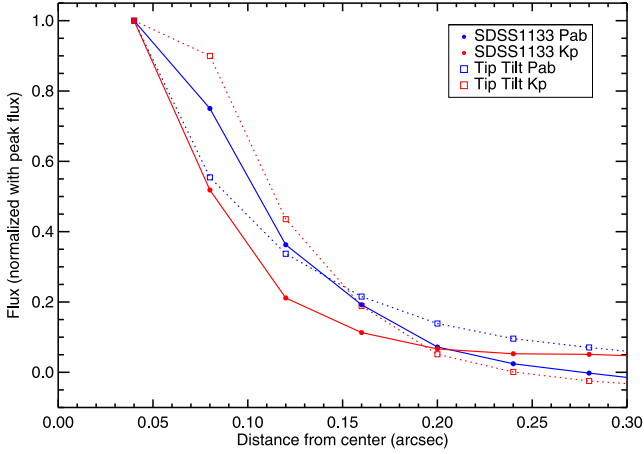
Figure 5. AO radial profiles of SDSS1133 (solid line) and the tip-tilt star (dashed line) used for PSF estimation in each observation. 0.1 arcsec corresponds to a physical scale of 14 pc. The radial profiles of the K_p (FWHM = 0.08 arcsec) and Paβ (FWHM = 0.15 arcsec) of SDSS1133 images are consistent with the stellar profiles of the tip-tilt stars.

$p = 0.92 \pm 0.27$ in 2003 (SDSS) and $p = 0.42 \pm 0.21$ in 2013 (Keck).

3.3 Host galaxy

SDSS1133 is located in Mrk 177, a nearby blue compact dwarf galaxy with peculiar morphology (Petrosian et al. 2007). The 5.8 arcsec separation between SDSS1133 and the centre of Mrk 177 corresponds to a projected physical distance of 0.81 kpc. Given the observed magnitude of $g = 15.69$ (SDSS), the galaxy absolute magnitude is $M_g = -16.6$, comparable to that of the Small Magellanic Cloud. The centre of the host galaxy was also observed

spectroscopically by SDSS, resulting in a measurement of the oxygen abundance, $12 + \log(O/H) = 8.58$, somewhat oxygen-rich given its brightness, but still on the SDSS mass–metallicity relation from Tremonti et al. (2004). In the host galaxy, Mrk 177, we measure the Ca II NIR triplet absorption lines to be within $3 \pm 10 \, \mathrm{km \, s^{-1}}$ of the redshift derived from the [O III] emission Line.

We can also measure the star formation rate (SFR) based on *GALEX* observations of Mrk 177 taken in 2004. Because of the low-spatial resolution of *GALEX*, we are unable to completely rule out the possibility of contamination by SDSS1133, but we measure an SFR of 0.05 $M_\odot$ yr^{-1} based on Kennicutt (1998).

4 DISCUSSION

Table 3 summarizes the unusual properties of SDSS1133. Given its long observed lifetime, luminosity, and highly variable behaviour, SDSS1133 is peculiar among AGNs, as well as among SNe, tidal disruption flares, ULXs, and other stellar phenomena. In the following sections, we discuss possible source scenarios for SDSS1133 in more detail. An LBV followed by an SN, or a recoiling SMBH, are the most likely scenarios, while a ULX, tidal flare, or tidally stripped AGN are disfavoured by the observations. Finally, we discuss the frequency of other events like SDSS1133.

4.1 LBV outburst, or LBV outburst followed by an SN

SDSS1133 is a source with an optical absolute magnitude of -13.5 (which could either be constant or caught serendipitously erupting in 1950, 1994, and 1999) followed by a brief, luminous transient in 2001/2002 that reached -16 mag and slowly faded to -13 mag. The value -13.5 mag exceeds the classical Eddington limit for a 100 $M_\odot$ star. The peak brightness of -16 is unprecedented for an LBV eruption, though there is still some debate about whether SN 2009ip and SN 1961V, both reaching

Figure 6. Optical diagnostic diagrams [N II]/Hα, [S II]/Hα, and [O I]/Hα versus [O III]/Hβ (e.g. Kewley et al. 2006) for SDSS1133 and the host galaxy Mrk 177 from the SDSS spectra. Lines indicate the approximate separation between H II regions, composite regions, Seyfert AGNs, and LINER AGNs.
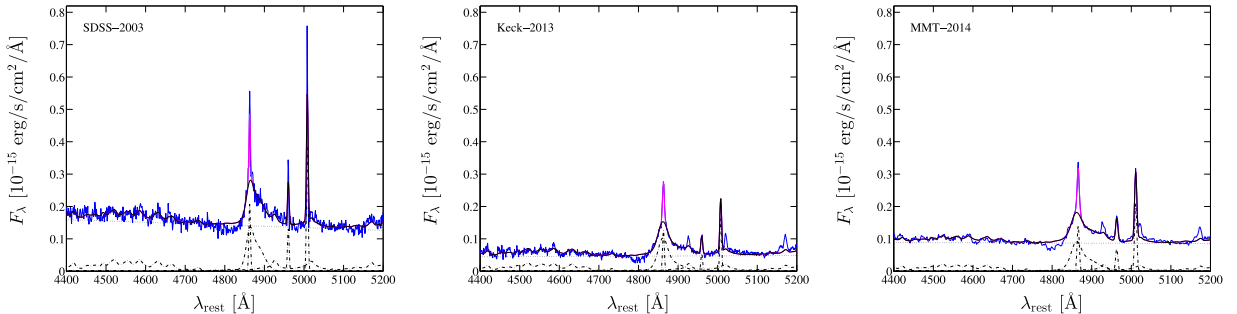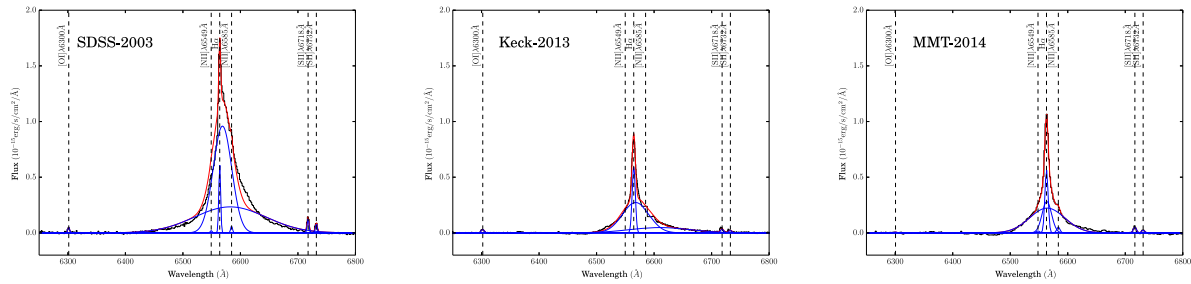

Figure 7. Left: fits to the Hβ region of SDSS1133 from 2003 (SDSS, left), 2013 (Keck, middle), and 2014 (MMT, right). The 2013 and 2014 spectra show narrow Fe II emission, weaker continuum emission, and a lower ratio of [O III] to Hβ compared to the 2003 spectrum.

Figure 8. Hα region of SDSS1133 from 2003 (SDSS, left), 2013 (Keck, middle), and 2014 (MMT, right). A power-law continuum has been subtracted from the spectra. Black lines indicate the observed spectra, blue lines are model components, and red lines represent the summed model spectra. Emission lines are shown at the redshift of the host galaxy Mrk 177.

nearly −18 mag in the optical, were extreme η Carinae-like events or core-collapse SNe (see also Kochanek, Szczygiel & Stanek 2011; Smith et al. 2011; Van Dyk & Matheson 2012). The closest LBV is η Car, which had a ÒGreat EruptionÓ in the mid-19th century that was ∼ −13.0 mag from 1843 to 1855, with some uncertainty from the historical records and estimated extinction (Smith & Frew 2011). Broad-line emission is also found in blue compact dwarfs (Izotov, Thuan & Guseva 2007) because of stellar winds around young massive stars (Izotov et al. 2007; Izotov, Thuan & Privon 2012) in regions of active star formation. However, stellar winds are ruled out for SDSS1133 since the Hα luminosity of 0.7×10^{40} erg s^{-1} is too large. A superbubble produced by multiple SNe is ruled out by the small spatial scale of the emission, <12 pc. As we discuss below, an LBV followed by an SN is a more likely scenario given the features of the recent optical spectra.

Late-time observations of interacting SNe provide critical information about the nature and mass-loss history of massive stars immediately before core collapse. The redshifted portion of the Hα and Hβ lines has become suppressed over the last decade, and the reddest individual peak has diminished in luminosity between 2003 and 2013. This could be dust in the post-shock medium that is obscuring emission from ejecta components in the receding hemisphere of the explosion (e.g. SN 2006jc; Smith, Foley & Filippenko 2008a). The Type IIn SN 1998S (Mauerhan & Smith 2012) does exhibit [O I], [O II], and [O III] emission 14 yr after outburst. Several SNe show ongoing broad emission as the fast SN ejecta cross the reverse shock behind the SN/CSM interface (e.g. SNe 1980K, 1993J, 1970G, and 1957D; Milisavljevic et al. 2012). Finally, the appearance of late-time narrow [Fe II] and [Ca II] in the 2013 spectra has been found in other SNe (e.g. SN 1992H; Filippenko 1997).

We can make a conservative order-of-magnitude estimate of the total bolometric luminosity of SDSS1133 over 12 yr based on the observed UV, optical, and NIR observations (2200–24,000 Å) to test whether it violates the total expected energy from an SN. To do this, we assume that the spectral energy distribution (SED) of SDSS1133 follows the last UV observation in 2013, the 2014 MMT optical spectrum (3675–8850 Å), and the *J* and K_p Keck measurements. We interpolate between the unobserved regions in the range 2200–24 000 Å. We assume that the SED follows the dashed lines in the *g*-band light curve in Fig. 2 and obtain a total energy of 1.7×10^{50} ergs. This is probably a lower limit since we exclude the far-UV and X-ray emission, and the bolometric correction is larger at earlier times because of the greater amounts of UV and X-ray emission. The largest amount of emission from an SN explosion thus far has been from SN 2003ma, with an integrated bolometric luminosity of 4×10^{51} ergs. While the integrated bolometric luminosity of SN 2003ma was a factor of ∼20 higher than for SDSS1133, the peak

emission of SN 2003ma was $M_R = -21.5$ mag, about 150 times brighter than SDSS1133.

The eruptive LBV and SN hypothesis has several issues that make SDSS1133 one of the most unusual LBV/SN candidates. The 51 yr putative eruptive LBV phase before the SN (whose peak brightness was in 2001) is the longest observed before an SN explosion. The luminous broad Hα emission requires interaction with a very dense CSM linked to an extreme amount of mass-loss by the LBV. A plot of Hα emission from SDSS1133 as a function of time after peak magnitude can be found in Fig. 11, as compared with the other most luminous SNe observed at late times. In 2013, SDSS1133 shows little decrease in Hα compared to other known SNe, and it has more luminous late-time Hα emission than even extreme cases like SN 1988Z (Aretxaga et al. 1999). Additionally, UV emission in SNe typically drops by several magnitudes in tens of days, while the UV emission of SDSS1133 exhibits no change when observed between 2004 by *GALEX* and 2013 by *Swift*. Strong UV emission is unexpected because SNe have line blanketing, and LBV eruptions usually form much dust. A possible explanation is a cluster of O-type stars or an H II region that is not detected in the NIR images. However, the NIR AO Paβ observations should directly trace the gas ionized by young, massive stars. In this case, the flux would be overestimated, which would reduce the pre-SN flux and the late-time fading. On the other hand, an H II region seems unlikely given the ∼22 pc resolution of AO in Paβ and the change in narrow-line emission between 2003 and 2013. Finally, additional monitoring is required to understand whether the light curve is consistent with a monotonic decrease expected from an SN. If the variability is confirmed to be non-monotonic, showing very significant rebrightening, scenarios for SDSS1133 with an LBV and SN origin will be severely constrained.

4.2 An AGN

4.2.1 Recoiling BH

While the SMBH occupation fraction in dwarf galaxies is only beginning to be constrained (e.g. Reines et al. 2013), any SMBH mergers that occur as a result of dwarf–dwarf mergers could produce a substantially offset recoiling AGN. This is because dwarf galaxies have low escape speeds, and thus even low-velocity recoil kicks may displace an SMBH from the galactic nucleus. If we assume that the potential of Mrk 177 is dominated by a dark-matter halo with an NFW profile (Navarro, Frenk & White 1996b) for its spatial mass distribution of dark matter and a halo to stellar-mass ratio of 30, then for the inferred stellar mass of $10^{8.55}$ M$_\odot$, a reasonable guess for the central escape speed is ∼170–200 km s^{-1}. The recent spectra have

Table 2. Emission-line properties.

Name[a]	Line	Offset[b] (km s^{-1})	FWHM[c] (km s^{-1})	Luminosity[d] (10^{36} erg s^{-1})	Date
Narrow lines					
SDSS1133	Hβ	26 ± 9	150	180 ± 8	2003
SDSS1133	Hβ	31 ± 15	220	94 ± 6	2013
SDSS1133	[O III] $\lambda5007$	26 ± 9	150	391 ± 3	2003
SDSS1133	[O III] $\lambda5007$	31 ± 15	220	170 ± 3	2013
SDSS1133	[O I] $\lambda6300$	26 ± 9	150	16 ± 6	2003
SDSS1133	[O I] $\lambda6300$	31 ± 9	220	22 ± 2	2013
SDSS1133	Hα	26 ± 9	150	211 ± 7	2003
SDSS1133	Hα	31 ± 9	220	335 ± 21	2013
SDSS1133	[N II] $\lambda6583$	26 ± 9	150	29 ± 2	2003
SDSS1133	[N II] $\lambda6583$	31 ± 9	220	15 ± 8	2013
SDSS1133	[S II] $\lambda6716$	26 ± 9	150	51 ± 6	2003
SDSS1133	[S II] $\lambda6716$	31 ± 9	220	27 ± 3	2013
SDSS1133	[S II] $\lambda6731$	26 ± 9	150	34 ± 6	2003
SDSS1133	[S II] $\lambda6731$	31 ± 9	220	19 ± 2	2013
SDSS1133	[Fe II] $\lambda7155$	19 ± 7	220	15 ± 2	2013
SDSS1133	[Ca II] $\lambda7291$	14 ± 4	220	46 ± 3	2013
SDSS1133	[Ca II] $\lambda7324$	8 ± 4	220	38 ± 3	2013
Broad lines					
SDSS1133	Hβ BLR	252 ± 43	1623 ± 144	554 ± 66	2003
SDSS1133	Hβ BLR	252 ± 43	1623 ± 144	441 ± 42	2013
SDSS1133	Hα BLR	330 ± 8	1254 ± 26	2335 ± 89	2003
SDSS1133	Hα VBLR	876 ± 28	4397 ± 72	4703 ± 201	2003
SDSS1133	Hα BLR	285 ± 5	2310 ± 13	1555 ± 17	2013
SDSS1133	Hα VBLR	1888 ± 38	6567 ± 67	862 ± 26	2013
SDSS1133	Hα BLR	38 ± 5	879 ± 35	578 ± 89	2014
SDSS1133	Hα VBLR	72 ± 8	3281 ± 532	1698 ± 342	2014
SDSS1133	O I $\lambda8446$	328 ± 36	647 ± 42	72 ± 16	2003
SDSS1133	O I $\lambda8446$	41 ± 5	262 ± 3	11 ± 2	2013
SDSS1133	Ca II $\lambda8498$	176 ± 22	643 ± 43	72 ± 15	2003
SDSS1133	Ca II $\lambda8498$	38 ± 6	264 ± 10	27 ± 3	2013
SDSS1133	Ca II $\lambda8452$	176 ± 22	640 ± 43	79 ± 10	2003
SDSS1133	Ca II $\lambda8452$	38 ± 4	265 ± 10	28 ± 3	2013
SDSS1133	Ca II $\lambda8662$	173 ± 22	631 ± 43	53 ± 11	2003
SDSS1133	Ca II $\lambda8662$	37 ± 4	265 ± 3	23 ± 3	2013
Host galaxy					
Mrk 177	Hβ	0	150	115 ± 9	2003
Mrk 177-IFU offset	Hβ	-18 ± 6	360	103 ± 35	2013
Mrk 177	[O III] $\lambda5007$	0	150	188 ± 4	2003
Mrk 177-IFU offset	[O III] $\lambda5007$	-18 ± 6	360	69 ± 25	2013
Mrk 177	[O I] $\lambda6300$	0	150	26 ± 5	2003
Mrk 177-IFU offset	[O I] $\lambda6300$	-18 ± 6	360	6 ± 3	2013
Mrk 177	Hα	0	150	332 ± 5	2003
Mrk 177-IFU offset	Hα	-18 ± 6	360	127 ± 17	2013
Mrk 177	[N II] $\lambda6583$	0	150	86 ± 5	2003
Mrk 177-IFU offset	[N II] $\lambda6583$	-18 ± 6	360	25 ± 8	2013
Mrk 177	[S II] $\lambda6716$	0	150	86 ± 5	2003
Mrk 177-IFU offset	[S II] $\lambda6716$	-18 ± 6	360	27 ± 11	2013
Mrk 177	[S II] $\lambda6731$	0	150	63 ± 5	2003
Mrk 177-IFU offset	[S II] $\lambda6731$	-18 ± 6	360	22 ± 11	2013

[a]Name of spectrum. Mrk 177 and SDSS1133 are from the SDSS. Mrk 177 IFU-offset is taken using the SNIFS IFU at the same radial offset from the nucleus of Mrk 177 as SDSS1133 (but in the opposite direction) and with the same aperture size. SDSS1133-IFU is taken of SDSS1133 with Mrk 177 IFU-offset subtracted, leaving only the broad lines to fit.
[b]Offset from the measured [O III] line in Mrk 177.
[c]All of the narrow lines measured were consistent with the instrumental resolution.
[d]Luminosity assuming a distance of 28.9 Mpc.

a broad Hα component consistent with little or no velocity offset; thus, in the recoiling AGN scenario we can assume that either the recoil kick was directed largely in the transverse direction or that the AGN is on a bound orbit near turnaround.

While high-velocity kicks (>1000 km s^{-1}) are expected to be quite rare, GW recoil velocities of 100–200 km s^{-1} should be relatively common. Lousto et al. (2012) calculate that, even if the progenitor SMBH spins are mostly aligned prior to their merger
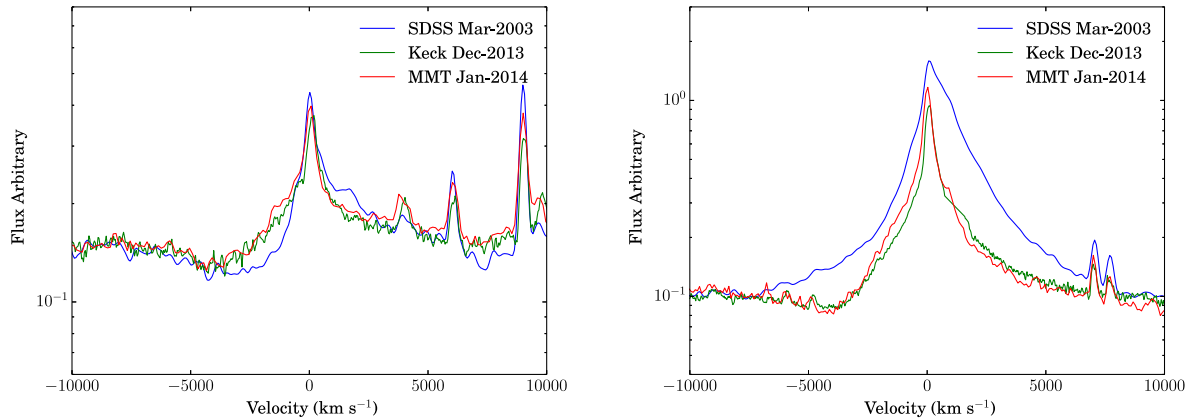
Figure 9. Broad-line region of SDSS1133 in Hβ (left) and Hα (right) from SDSS in 2003, Keck in 2013, and the MMT in 2014. The spectra have been smoothed to the same spectral resolution, offset to the same continuum level, and plotted on a log scale in the ordinate. There is evidence of blueshifed absorption in the Hβ and Hα regions at -3000 to $-8000 \, \mathrm{km \, s^{-1}}$ in almost all of the spectra except the 2003 SDSS spectra. The total broad Hβ emission dropped by 10–20 per cent between 2003 and 2013–2014, whereas the total broad Hα emission dropped by 65–70 per cent.
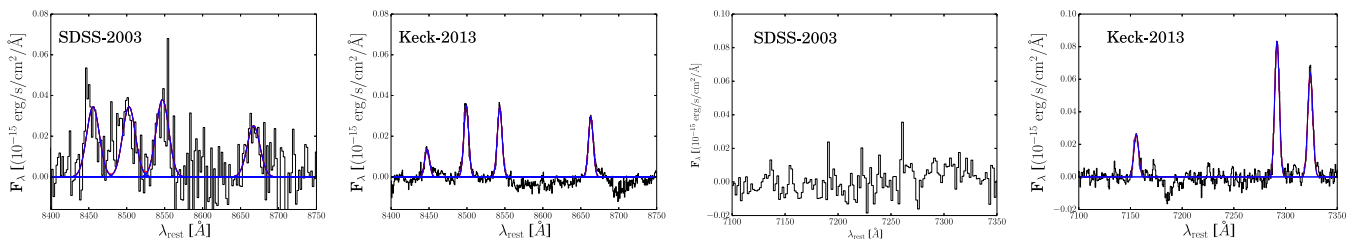
Figure 10. Calcium near-IR triplet region of SDSS1133 as observed in 2003 (left) and 2013 (middle left), showing line fits to O I λ8446 and Ca II λλ8498, 8452, 8662. The 2003 spectra shows broader emission. Fits to [Fe II] λ7155 and [Ca II] λλ7291, 7324 in 2003 (middle right) and 2013 (right) are also shown. No emission lines are detected in 2003, whereas the 2013 spectrum exhibits strong, narrow emission consistent with the resolution of the instrument (220 $\mathrm{km \, s^{-1}}$).

Table 3. Source properties.

Property[a]	AGN	LBV Outburst	SNe
Bright (> -13 mag) optical emission for 51 yr	Y	Y	
Optical drop of 2.2 mag in 1 yr	R	Y	Y
Peak optical mag of -16	Y		Y
<20 pc point-source emission	Y	Y	Y
Constant UV emission for a decade	Y		
Constant $g - i$ colour for a decade	Y		
Changing broad-line width	Y		Y
Broad Hα ($>1000 \, \mathrm{km \, s^{-1}}$) for a decade	Y		R
Broad-line Balmer decrement change	R		Y
Narrow [O III] emission	Y		R
Late-time narrow [Fe II] emission	R		R
Late-time narrow [Ca II] emission	R		R
P-Cygni blueshifted absorption	R		Y
$i - K_p$ colour $= 2.5$ mag	Y		R
0.3–10 keV/Hα ratio ≈ 1	R		Y

[a]R indicates rarely, Y indicates common, and blank indicates never observed among this type of source.

(thus reducing the kick speed), 100–200 $\mathrm{km \, s^{-1}}$ kicks should be produced in 21–28 per cent of SMBH mergers (assuming a cosmologically motivated distribution of SMBH mass ratios). These would correspond to bound or marginally unbound recoil kicks. An additional 12–13 per cent of such mergers should result in recoil velocities of 200–300 $\mathrm{km \, s^{-1}}$, which would leave the recoiling AGN unbound from its host.

The accretion rate on to a recoiling AGN should decrease monotonically with time as its accretion disc diffuses outwards (unless the SMBH encounters a fresh fuel supply). Thus, even if the SMBH was accreting at the Eddington limit at the time of the kick, its accretion rate may be only a few per cent of Eddington by the time it is observed as an offset AGN, several Myr later. This is consistent with the low AGN luminosity observed for SDSS1133. Note that typical offset AGN lifetimes are a few to a few tens of Myr (Blecha et al. 2011), consistent with the inferred travel time for an SMBH from the centre of Mrk 177 to the current offset (0.8 kpc) of SDSS1133, and allowing for some deceleration.
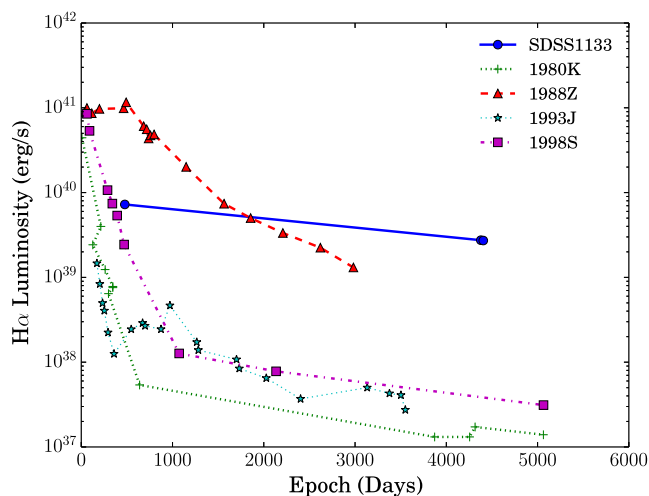
Figure 11. Hα emission from SDSS1133 compared to the most luminous late-time SNe from the literature (Aretxaga et al. 1999; Chandra et al. 2009; Mauerhan & Smith 2012). SDSS1133 displays a very flat profile along with the brightest late-time Hα ever seen, even including very luminous SNe such as SN 1988Z.

Furthermore, if the recoiling SMBH is on a bound orbit, it may be able to replenish its fuel supply on subsequent passages through the galaxy, thus extending its offset AGN lifetime (Blecha et al. 2011).

While the expected properties of recoiling AGNs are poorly understood, SDSS1133 does show many features similar to observed broad-line AGN and those expected for recoiling AGNs, including the following: (1) point-like emission for 63 yr that is on very small scales of $\lesssim 12$ pc, (2) broad Fe II emission is seen in almost all Type-1 AGN spectra, (3) broad Ca II NIR triplet emission is found in 1/3 of quasars (Netzer 1990), (4) a blue power-law continuum with no detected stellar absorption lines from the host-galaxy nucleus, (5) some narrow-line optical emission-line diagnostics consistent with an AGN, (6) an SMBH mass measurement that remains constant within the uncertainties over a decade, despite changes in the continuum, (7) variability with dimming and rebrightening, (8) lack of significant colour evolution, (9) relatively constant UV luminosity, and (10) Hα luminosity consistent with a low-mass SMBH accreting at a typical rate of a few per cent of $L_{\rm Edd}$.

Since the majority (∼80–100 per cent) of AGNs are variable (MacLeod 2012), and less luminous AGNs tend to be more variable (Desjardins, Sarajedini & vanden Berk 2007), one might expect SDSS1133 to show high variability. However, the drop in brightness of SDSS1133 between the last SDSS image on 2002 April 1 and the SDSS spectra taken on 2003 March 9, over a period of about a year, is quite large at 2.2–2.9 mag. While this sharp a change has been observed in a few AGNs (e.g. Gaskell 2006), the large variability and strong late-time UV emission are more consistent with tidal flares.

As an AGN, the rapid drop in luminosity between 2002 and 2003, the narrow [Fe II] lines, and the presence of [Ca II] λλ7291, 7324 emission are difficult to understand. The [Ca II] lines are rarely seen in AGNs because dust grains are presumed to suppress the Ca II emission through the substantial Ca depletion (Ferland 1993). While found in some AGNs such as I Zw 1 (Phillips 1976), the feature is rare among AGN spectra.

The total broad Hα luminosity of 0.7×10^{40} erg s^{-1} would make this a very low luminosity AGN, with a predicted bolometric

luminosity of ∼10^{42} erg s^{-1} (Greene & Ho 2007) and an Eddington ratio of 0.02. Thus, this object is similar in its gross properties to many of the very low luminosity AGNs recently discovered, which have inferred BH masses in the 10^5–10^6 M$_\odot$ range (Reines et al. 2013).

Finally, in a variant of the recoiling AGN scenario, the extreme variability of SDSS1133 could arise from the tidal disruption of a star by the recoiling BH. This would result in a short-lived, luminous flare from the accretion of the stellar debris. Tidal disruption events are bright in the X-rays, UV, and sometimes optical (Komossa 2002; Gezari et al. 2006). For low-mass SMBHs such as SDSS1133, the flare is expected to be super-Eddington, with an estimated duration of ∼2–5 yr (Ulmer 1999). Stellar tidal disruptions by recoiling SMBHs may contribute a small but non-negligible fraction to the total rate of tidal disruptions by SMBHs (Komossa & Merritt 2008; Stone & Loeb 2012).

Because SDSS1133 is detected over 63 yr, with roughly constant luminosity and broad-line emission over the past decade, this scenario requires the SMBH to have a reservoir of gas persisting before and after the event, which produces continuous AGN emission. Since the 2003 spectrum does not show any distinct features expected from tidal disruption flares (e.g. Strubbe & Quataert 2011), we conclude that any such flare must have faded in <2 yr from observed peak brightness. This, combined with the small decline in brightness during the 104 d between the 2001 and 2002 observations, argues against the tidal disruption scenario. More fundamentally, this scenario requires an additional rare event (a tidal disruption flare) in a highly unusual object, namely a recoiling BH in a dwarf galaxy.

4.2.2 An infalling tidally stripped dwarf or ULX?

It is theoretically possible that Mrk 177 is observed in an earlier stage of merging, such that SDSS1133 originated in a satellite galaxy falling into the host galaxy. In this case, the centre of the host galaxy could contain its own, relatively quiescent SMBH. The AO images in the K_p and Paβ bands both show an unresolved point source at the location of SDSS1133 down to spatial scales of 12 and 22 pc, respectively. This is consistent with a recoiling AGN that has left its host galaxy behind. If instead SDSS1133 is an infalling dwarf galaxy, then it must have been tidally stripped at radii >12 pc, a strong constraint. Numerical models suggest that repeated strong tidal encounters with a much more massive host can remove more than 99 per cent of the total initial mass of a satellite galaxy (e.g. Peñarrubia, Navarro & McConnachie 2008). However, the only galaxy near SDSS1133 is Mrk 177, a dwarf galaxy with insufficient mass to be responsible for such extreme tidal stripping of a fellow dwarf companion.

When an SMBH is present, its sphere of influence sets an upper limit on the amount of stripping; even strong tidal encounters will be ineffective at removing mass where the SMBH dominates the gravitational potential. Making the first-order assumption that the dwarf galaxy followed the observed SMBH-bulge scaling relations prior to stripping, our SMBH mass estimate of $10^{6.0}$ M$_\odot$ for SDSS1133 implies a stellar velocity dispersion of 60 km s^{-1} (Tremaine et al. 2002). Using the standard definition for the size of the SMBH sphere of influence, $r_{\rm infl} = GM_{\rm BH}/\sigma_*^2$, we find $r_{\rm infl} \approx 1$ pc. This implies that the SMBH sphere of influence is likely to be unresolved, such that a tidal dwarf remnant stripped to within a few times $r_{\rm infl}$ cannot be ruled out. Note that extrapolation from the SMBH-bulge scaling relations (Häring & Rix 2004) implies a

progenitor galaxy for SDSS1133 *larger* than Mrk 177. However, the value of σ_* inferred from Tremaine et al. (2002) is likely an upper limit. Tidal stripping and stellar feedback can decrease the velocity dispersion (e.g. Navarro, Eke & Frenk 1996a; Peñarrubia et al. 2009; Zolotov et al. 2012), and the progenitor may also have been somewhat less massive. All of these would yield a larger radius of influence. Specifically, a factor of 4 decrease in velocity dispersion from the above estimates would imply that the SMBH sphere of influence is at least marginally resolvable ($r_{infl} \approx 7$–19 pc). Therefore, the tidal stripping scenario is very strongly constrained by the need for both an unidentified massive galaxy to strip the SDSS1133 progenitor and for a compact, unresolvable SMBH sphere of influence.

In contrast, a recoiling SMBH ejected from a spherical stellar distribution will only retain stars within a radius $r \approx (\sigma_*/v_k)^2 \, r_{infl}$. For a Bahcall–Wolf profile normalized such that $M(r < r_{infl}) = 2M_{BH}$ (Bahcall & Wolf 1976), a kick of 200 km s^{-1} would only allow the inner 0.003 pc of the stellar cusp, or a few thousand M$_\odot$, to remain bound to the SMBH. Thus, in the recoil scenario the stellar cusp would not be resolved under any circumstances.

Interpreting SDSS1133 as a ULX, it is either accreting ambient gas (i.e., indistinguishable from an AGN discussed in previous scenarios) or accreting from a stellar companion (which is untenable for our large inferred BH mass 10^6 M$_\odot$). The most extreme ULX is HLX-1 (ESO 243-49), with $L_X = 2 \times 10^{42}$ erg s^{-1} and a BH mass of $(3$–$300) \times 10^3$ M$_\odot$ (Farrell et al. 2009), making it the most convincing example of an IMBH. This BH mass is significantly lower than that inferred for SDSS1133. HLX-1 is offset from its host-galaxy centre by $\sim$3 kpc (in projection), and may reside in a tidally stripped dwarf galaxy that is merging with the host galaxy (e.g. Mapelli, Zampieri & Mayer 2012). In principle, the AGN in SDSS1133 could have a similar origin, such that its host galaxy was tidally stripped long ago, but the point-like AO observations and lack of nearby massive galaxies place strong constraints against this. If SDSS1133 were a ULX, it would be the first ever to be observed with broad Balmer lines (Roberts et al. 2011). Given the inferred BH mass of SDSS1133, as a ULX it is extremely X-ray weak, with a 2–10 keV to *V*-band flux ratio of $\sim$100; this is below that of most ULXs, though some in their low states such as M101-ULX1 and M81-ULX1 have observed ratios similar to this (Tao et al. 2012).

4.3 Frequency of objects like SDSS1133

A survey of all 3579 low-redshift ($z < 0.3$) broad emission-line objects (>1000 km s^{-1} FWHM; Stern & Laor 2012) found only two objects offset from the host-galaxy nucleus: SDSS1133 along with a very close dual AGN Mrk 739 (Koss et al. 2011). The low frequency of detections of spatially offset broad-line sources found in the SDSS quasar survey (1/3579, <0.1 per cent) does not exclude the possibility of a significant population. The small physical separation of 800 pc found for SDSS1133 can only be resolved at very low redshift with the imaging of the SDSS (at $z < 0.03$, 1.3 arcsec $\approx$ 800 pc). The broad-line luminosity of SDSS1133 is among the weakest dozen of the SDSS sample, and at the current reduced brightness of SDSS1133 it would be too faint for the survey (Richards et al. 2004). Future space-based surveys such as *Euclid* and *WFIRST* will obtain high-resolution images with precision astrometry of large areas of the sky, enabling them to probe the nuclear regions of nearby galaxies for offset point sources. Both have IR grisms as part of their wide-field surveys to cover broad AGN lines in the NIR such as the Paschen lines.

5 CONCLUSION

SDSS1133 has many observed properties consistent with a recoiling AGN, but it also has some properties that favour interpretation of this source as an eruptive LBV star outbursting for decades followed by a Type IIn SN. SDSS1133 would be the longest LBV eruption ever observed and have a much greater late-time Hα luminosity than even extreme events like SN 1988Z. SDSS1133 has recently undergone a 1 mag rebrightening in PS1 images, suggesting that the coming years will be critical to understand the true nature of this source. Future high-spatial resolution and high sensitivity UV, X-ray, and radio observations of SDSS1133 are critical for constraining the source nature. In the UV, the measurement of strong N V λ1240 and (especially) broad C IV λ1550 emission would decisively favour the AGN interpretation. Additionally, high-resolution UV images could determine whether the strong UV emission and prominent narrow-line emission in [O I], [O II], and [O III] is produced by a compact H II region or a young star cluster not seen in the NIR AO image. High-sensitivity X-ray observations could differentiate between softer thermal X-ray emission from an SN shock and an AGN power law.

REFERENCES

Aldering G. et al., 2006, ApJ, 650, 510
Aretxaga I., Benetti S., Terlevich R. J., Fabian A. C., Cappellaro E., Turatto M., della Valle M., 1999, MNRAS, 309, 343
Bahcall J. N., Wolf R. A., 1976, ApJ, 209, 214
Bekenstein J. D., 1973, ApJ, 183, 657
Blecha L., Loeb A., 2008, MNRAS, 390, 1311
Blecha L., Cox T. J., Loeb A., Hernquist L., 2011, MNRAS, 412, 2154
Blecha L., Civano F., Elvis M., Loeb A., 2013, MNRAS, 428, 1341
Campanelli M., Lousto C. O., Zlochower Y., 2006, Phys. Rev. D, 74, 084023
Chandra P., Dwarkadas V. V., Ray A., Immler S., Pooley D., 2009, ApJ, 699, 388
Chevalier R. A., Fransson C., 1994, ApJ, 420, 268
Civano F. et al., 2010, ApJ, 717, 209
Civano F. et al., 2012, ApJ, 752, 49
Desjardins T. D., Sarajedini V. L., vanden Berk D. E., 2007, BAAS, 39, 802
Farrell S. A., Webb N. A., Barret D., Godet O., Rodrigues J. M., 2009, Nature, 460, 73
Ferland G. J., 1993, in Beckman J., Luis C., Hagai N., eds, The Nearest Active Galaxies. Consejo Superior de Investigaciones Cientificas, Madrid, p. 75
Filippenko A. V., 1989, AJ, 97, 726
Filippenko A. V., 1997, ARA&A, 35, 309
Forbes D. A., Lasky P., Graham A. W., Spitler L., 2008, MNRAS, 389, 1924
Gal-Yam A. et al., 2007, ApJ, 656, 372
Gaskell C. M., 2006, in Gaskell C. M., McHardy I. M., Peterson B. M., Sergeev S. G., eds, ASP Conf. Ser. Vol. 360, AGN Variability from X-Rays to Radio Waves. Astron. Soc. Pac., San Francisco, p. 111
Gezari S. et al., 2006, ApJ, 653, L25
Graur O., Maoz D., 2013, MNRAS, 430, 1746
Greene J. E., Ho L. C., 2007, ApJ, 667, 131
Grier C. J. et al., 2013, ApJ, 773, 90
Häring N., Rix H.-W., 2004, ApJ, 604, L89
Izotov Y. I., Thuan T. X., Guseva N. G., 2007, ApJ, 671, 1297
Izotov Y. I., Thuan T. X., Privon G., 2012, MNRAS, 427, 1229
Jonker P. G., Torres M. A. P., Fabian A. C., Heida M., Miniutti G., Pooley D., 2010, MNRAS, 407, 645
Keel W. C. et al., 2012, MNRAS, 420, 878
Kennicutt R. C., 1998, ApJ, 498, 541
Kewley L. J., Groves B., Kauffmann G., Heckman T., 2006, MNRAS, 372, 961
Kiewe M. et al., 2012, ApJ, 744, 10
Kochanek C. S., Szczygiel D. M., Stanek K. Z., 2011, ApJ, 737, 76
Komossa S., 2002, in Gilfanov M., Sunyaev R., Churazov E., eds, Proc. MPA/ESO/MPE/USM Joint Astron. Conf., Lighthouses of the Universe: The Most Luminous Celestial Objects and Their Use for Cosmology. Springer-Verlag, Berlin, p. 436
Komossa S., 2012, Adv. Astron., 2012, 14
Komossa S., Merritt D., 2008, ApJ, 689, L89
Koss M. et al., 2011, ApJ, 735, L42

López-Corredoira M., Gutiérrez C. M., 2006, in Lerner E. J., Almeida J. B., eds, AIP Conf. Ser. Vol. 822, First Crisis in Cosmology Conference. Am. Inst. Phys., New York, p. 75
Lousto C. O., Zlochower Y., 2011, Phys. Rev. Lett., 107, 231102
Lousto C. O., Zlochower Y., Dotti M., Volonteri M., 2012, Phys. Rev. D, 85, 84015
MacLeod C. L., 2012, PhD thesis, Univ. Washington
Madau P., Quataert E., 2004, ApJ, 606, L17
Mapelli M., Zampieri L., Mayer L., 2012, MNRAS, 423, 1309
Mauerhan J., Smith N., 2012, MNRAS, 424, 2659
Mauerhan J. C. et al., 2013, MNRAS, 430, 1801
Merritt D., Milosavljević M., 2005, Living Rev. Relativ., 8, 8
Milisavljevic D., Fesen R. A., Chevalier R. A., Kirshner R. P., Challis P., Turatto M., 2012, ApJ, 751, 25
Navarro J. F., Eke V. R., Frenk C. S., 1996a, MNRAS, 283, L72
Navarro J. F., Frenk C. S., White S. D. M., 1996b, ApJ, 462, 563
Netzer H., 1990, in Courvoisier T. J.-L., Mayor M., eds, Saas-Fee Advanced Course 20 of the Swiss Society for Astrophysics and Astronomy: Active Galactic Nuclei. Springer-Verlag, Berlin, p. 57
Ofek E. O. et al., 2014, ApJ, 789, 104
Peñarrubia J., Navarro J. F., McConnachie A. W., 2008, ApJ, 673, 226
Peñarrubia J., Navarro J. F., McConnachie A. W., Martin N. F., 2009, ApJ, 698, 222
Peng C. Y., Ho L. C., Impey C. D., Rix H.-W., 2002, AJ, 124, 266
Peres A., 1962, Phys. Rev., 128, 2471
Peth M. A., Ross N. P., Schneider D. P., 2011, AJ, 141, 105
Petrosian A., McLean B., Allen R. J., MacKenty J. W., 2007, ApJS, 170, 33
Phillips M. M., 1976, ApJ, 208, 37
Reines A. E., Greene J. E., Geha M., 2013, ApJ, 775, 116
Richards G. T. et al., 2001, AJ, 121, 2308
Richards G. T., Hall P. B., Strauss M. A., vanden Berk D. E., Schneider D. P., Reichard T. A., 2004, in Mújica R., Maiolino R., eds, Proc. Guillermo Haro Conf. 2003, Multiwavelength AGN Surveys. Princeton Univ. Press, Princeton, NJ, p. 46
Roberts T. P., Gladstone J. C., Goulding A. D., Swinbank A. M., Ward M. J., Goad M. R., Levan A. J., 2011, Astron. Nachr., 332, 398
Schlafly E. F., Finkbeiner D. P., 2011, ApJ, 737, 103
Sesana A., 2013, New J. Phys., 15, 073035
Shen Y., 2013, Bull. Astron. Soc. India, 41, 61
Sijacki D., Springel V., Haehnelt M. G., 2011, MNRAS, 414, 3656
Smith N., Frew D. J., 2011, MNRAS, 415, 2009
Smith N., Foley R. J., Filippenko A. V., 2008a, ApJ, 680, 568
Smith N., Chornock R., Li W., Ganeshalingam M., Silverman J. M., Foley R. J., Filippenko A. V., Barth A. J., 2008b, ApJ, 686, 467
Smith N. et al., 2009, ApJ, 695, 1334
Smith N., Li W., Silverman J. M., Ganeshalingam M., Filippenko A. V., 2011, MNRAS, 415, 773
Stern J., Laor A., 2012, MNRAS, 423, 600
Stone N., Loeb A., 2012, MNRAS, 422, 1933
Strubbe L. E., Quataert E., 2011, MNRAS, 415, 168
Tao L., Feng H., Kaaret P., Grisé F., Jin J., 2012, ApJ, 758, 85
Thorne K. S., Braginskii V. B., 1976, ApJ, 204, L1
Trakhtenbrot B., Netzer H., 2012, MNRAS, 427, 3081
Tremaine S. et al., 2002, ApJ, 574, 740
Tremonti C. A. et al., 2004, ApJ, 613, 898
Tully R. B., 1994, VizieR On-line Data Catalog, 7145, 0
Ulmer A., 1999, ApJ, 514, 180
Van Dyk S. D., Matheson T., 2012, ApJ, 746, 179
Veilleux S., Osterbrock D. E., 1987, ApJS, 63, 295
Volonteri M., 2007, ApJ, 663, L5
Zhou H., Wang T., Yuan W., Lu H., Dong X., Wang J., Lu Y., 2006, ApJS, 166, 128
Zolotov A. et al., 2012, ApJ, 761, 71